GROUND DEMONSTRATION OF HYPERTELESCOPES

S. Gillet[1], P. Riaud[1,2], O. Lardière[1], J. Dejonghe[3], A. Labeyrie[1,3], V. Borkowski[1], and L. Arnold[4]

[1]L.I.S.E. Observatoire de Haute Provence 04870 Saint Michel l'Observatoire
sgohp@obs-hp.fr, lardiere@obs-hp.fr, labeyrie@obs-hp.fr, borkowski@obs-hp.fr
[2]L.E.S.I.A. Observatoire de Meudon Place Jules Janssen, F-92195 Meudon Cedex
pierre.riaud@obspm.fr
[3]Collège de France, 11 place Marcelin Berthelot, 75005 Paris
dejonghe@obs-hp.fr
[4]O.H.P. Observatoire de Haute Provence 04870 Saint Michel l'Observatoire
arnold@obs-hp.fr

ABSTRACT

We have built a 10 cm diameter interferometer having 78 apertures of 1 mm diameter and using a direct snapshot imaging mode : the pupil densification also called hypertelescope. We have tested the direct snapshot performance of this hypertelescope with laboratory simulated multiple stars and on the sky. Characterizations of our hypertelescope limited science results but this test offers interesting perspectives for the future on the ground and in space. Densification may have applications in various fields such as providing a similar limiting magnitude but with a significantly increased angular resolution compared to a monolithic telescope with a same collecting surface.

Key words: direct imaging interferometers; hypertelescope; high angular resolution; binary star.

1. INTRODUCTION

We present results obtained with a multi-aperture densified-pupil imaging interferometer or hypertelescope. Interferometry can provide various trade-offs between angular resolution and collecting area, but snapshot imaging may often improve observations and data collecting. In 1996, Labeyrie (1996) described an optical architecture allowing direct high-resolution imaging with high contrast. Pedretti et al. (2000) tested a first method of densification, using a diffractive approach. We describe here an improved optical scheme using a pair of micro-lens arrays for achieving the pupil densification. This miniature hypertelescope was tested on bright binary stars. We present here the results obtained on the sky.

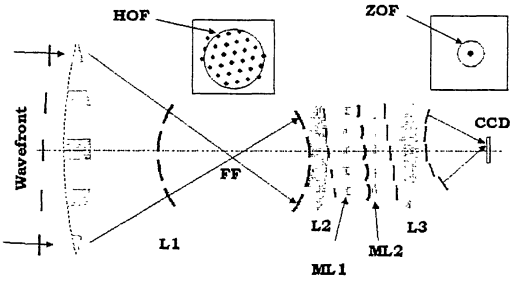

Figure 1. A giant segmented lens L1 simulates the entrance optics. The incoming flat wavefront from an off-axis star focuses at the Fizeau focus (FF), forming the multi-peaked diffraction pattern sketched above. Once densified, the wavefront average shape remains flat and parallel but becomes stair-shaped since the slope of each wavefront segment is reduced by the pair of micro-lenses introducing identical propagation delays. The resulting wavefront is finally a stair-shaped wavefront with an unaffected average slope and focuses to a single narrow interference peak at the center of the broader diffraction pattern from each sub-pupil.

2. HYPERTELESCOPE PRINCIPLE

A classical multi-aperture interferometer with a periodic array of N small mirrors separated by the distance s can provide direct images. But if the spacing of the sub-apertures becomes much larger than their size, the image quality, in terms of its luminosity and the data analysis is considerably affected. The resulting image at the Fizeau focus (FF) has a low contrast central peak surrounded by a large number of secondary dispersed peaks (see Fig.1). The degradation is caused by the diffractive spreading of light from each small sub-aperture, generating a halo much broader than the central interference

Proc. ESLAB 36 Symposium, 'Earth-Like Planets and Moons', ESTEC, Noordwijk, 3-8 June 2002 (ESA SP-514, October 2002)

peak and taking most light away from it. Several attempts to improve snapshot images by changing the entrance sub-apertures position have come up against the golden rule (Traub W.A. (1986)) : any recombination of the entrance pupil destroys the image's properties. This latter rule was in fact to much restrictive as demonstrated by Labeyrie (1996). Recombination of the entrance sub pupils is possible if the geometrical pattern formed by the center of each mirror is kept. If care is taken to configure the exit pupil so that sub-pupil centers be arranged like in the entrance aperture, a direct image is obtainable with full luminosity. The resulting densified image is a "windowed convolution" of the object : the normal convolution of the object with a spread-function, the "interference" function is followed by a multiplication by a "window" function which is the diffraction pattern from a single exit sub-pupil (Fig.2). This window function defines a small region

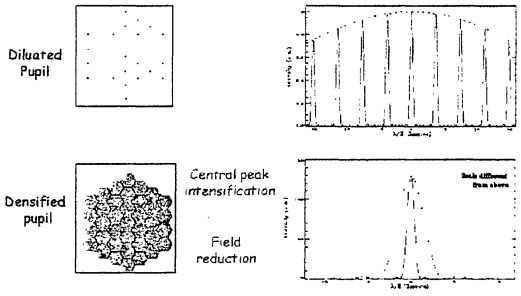

Figure 2. The upper figure shows a Fizeau interferometer, with left, the diluted entrance pupil and right, the resulting image for a point source containing more than hundred peaks with low intensities. Above, the figures represents the same entrance pupil but densified : the central peak is intensified but the field of view (window function) shrinks significantly compared to a non densified case.

of the sky, where the densified image of a star appears as a white central peak. Outside this region, the image of the star appears dispersed. Following Gillet et al (2001), we call ZOF (Zero Order Field) this narrow usable field and HOF (High Order Field) the peripheral sky field of size λ/d where d is the size of one sub-aperture :

$$ZOF(sky) = \frac{\lambda}{d.\gamma_D} \qquad (1)$$

where γ_D is the densification ratio defined by:

$$\gamma_D \equiv \frac{\left(\frac{D}{d}\right)_i}{\left(\frac{D}{d}\right)_o} = \frac{d_o}{d_i} \quad if\ D_i = D_o \qquad (2)$$

D_i and D_o the entrance and exit baselines, d_i and d_o are the entrance and exit mirror diameters.

When a star moves off axis, its corresponding dispersed peak begins to appear at the opposite edge of the sub-aperture's Airy disk. Thus, any point source outside the ZOF is still imaged through its dispersed peak. For a square periodic array, the number of resolved elements in the ZOF is 4N, where N is the number of sub-apertures.

3. EXPERIMENTAL SETUP AND RESULTS

Following numerical simulations and a first experimented hypertelescope using a diffraction based densification method (Pedretti et al. (2000)), we tried to improve the image and densification quality. We

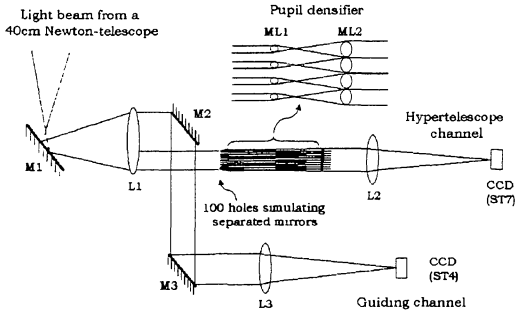

Figure 3. Hypertelescope experimental setup. The incoming light beam from a Newtonian telescope is collimated by lens L1. A Fizeau mask installed for convenience in the pupil plane following L1, rather than at the primary mirror, has N = 78 holes of 100μm size each. It defines in the entrance aperture a virtual "diluted giant mirror" of 10 cm size with s= 1 mm sub-apertures.

made a miniature hypertelescope with 10 cm baseline in order to have nearly diffraction-limited image quality without adaptive optics. A lens L1 (Fig.3) produces a pupil image, 10 times smaller than the entrance aperture, which is masked by a grid of 78 holes of 0.1 mm size, centered 1 mm apart. The virtual grid thus defined in the entrance aperture has 1 mm holes spaced 10 mm apart on the sky. Two arrays of convergent and confocal micro-lenses (ML1 and ML2) achieve the pupil densification. Collimated beams from each sub-pupil become recollimated and widened when transmitted through the facing pair of micro-lenses. The densification factor, ratio of ML2 and ML1's focal lengths, provides 80 % filling (diameter) in the exit pupil ($\gamma_D = 6$). The micro-lens arrays utilized were fabricated with enough lens-to-lens uniformity of thickness to keep piston errors within Rayleigh's tolerance, as required for a highly constructive interference, providing a high Strehl ratio, in the star's "high-resolution" image.

The main hypertelescope characterizations are described on table 1. With its aperture size of 10 cm and equivalent mirrors of 1 mm diameter, the ZOF extent is $1.22(\lambda/d)/\gamma_D = 28''$ at $\lambda = 650$ nm and the angular resolution is $\lambda/B = 1.34''$.

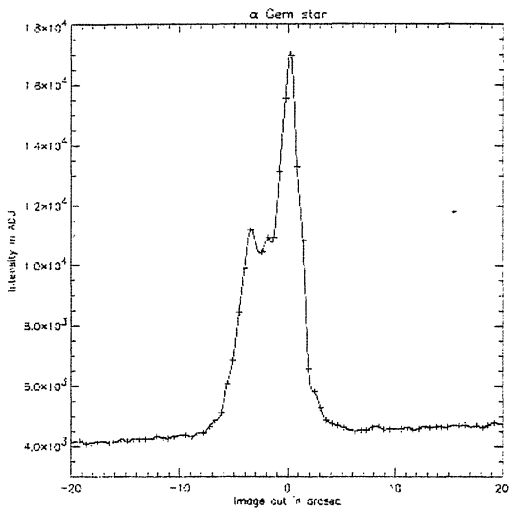

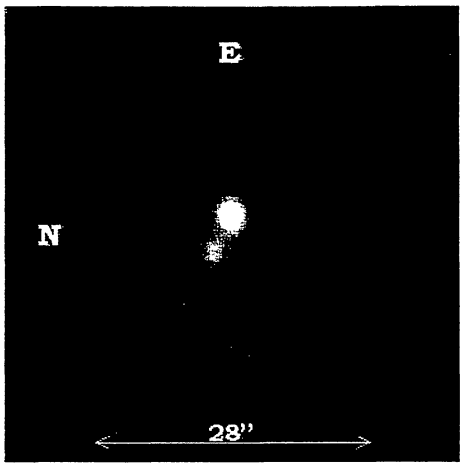

Figure 4. Image of Castor and its profil, showing the resolved binary A-B, spaced 3.8 arc-second. The ZOF diameter is about 28 arcsec wide.

The experimental setup required some preliminary laboratory testing. The micro-lens arrays were aligned with a He-Ne laser. Unlike the first hypertelescope which used diffraction (Pedretti et al. (2000)), we experienced a critical point with the rotational alignment of the micro-lens arrays which requires a precision of less than 1°. The final image has then a central white peak surrounded by several secondary dispersed peaks if densification is not completely achieved. Once the alignment was completed, we have tested the imaging capabilities of the hypertelescope with laboratory simulated multiple stars. Figure 5 shows the laboratory images

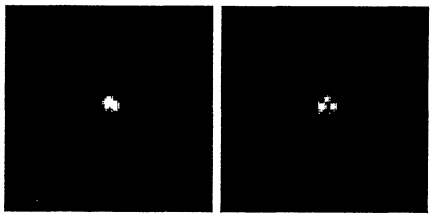

Figure 5. Laboratory simulated double (left) and triple (right) star observed with the hypertelescope. The image is a color composite of three images taken through R,G and B filters.

Table 1. Hypertelescope characteristics.

Parameters	Values
Hypertelescope size B	10 cm disk
Number of sub-apertures	78
Mirror size (entrance/exit)	1 mm/100 μm
Spacing s (sky)	10 mm
Collecting surface	78.5 mm^2
ML_1 focal length	20 mm
ML_2 focal length	120 mm
Densification ratio	6 (80 %)
Field of view (ZOF)	28 arcsec
Angular resolution	1.34 arcsec @ 0.65μm
Spectral range	450 to 750 nm
Image sampling	0.62 pixel/arcsec

obtained with equivalent R, G and B filters. These preliminary results are in good agreement with theory in terms of flux concentration and field of view for the ZOF. In a second step, we assessed the hypertelescope's capabilities on bright stars. On Fig.4 we show Castor (α *Gem*), of magnitude $m_v = 1.98$. The magnitude difference with it's brightest companion is $\Delta m = 0.9$. Exposures were taken with and without the Wratten filters WR(25), WV(58) and WB(80A). The four residual peaks surrounding the central one result from the uncomplete densification utilized, 80%. The exposure times varied from 10 to 30 min. On Fig.(5) the companion of α *Gem* appears clearly. We measured for JD=2452193.67 a separation $\rho = 3.8$ and an angle $\alpha = 68.2°$. The literature gives (Heintz (1988)), for this date $\rho = 4.0$ arcsec and $\alpha = 63.81°$.

Table 2. Hypertelescope measurements on Castor

	measured value	expected value
Separation r (arcsec)	3.8 ± 0.3	4
Position angle a (°)	68.2 ± 5	63.81
Δm (Castor A-Castor B)	0.8 ± 0.15	0.9

4. EXAMPLE OF A GROUND BASED HYPERTELSCOPE

As sketched in Fig.6, the Carlina approach is inspired form Arecibo's radio-telescope. It uses the

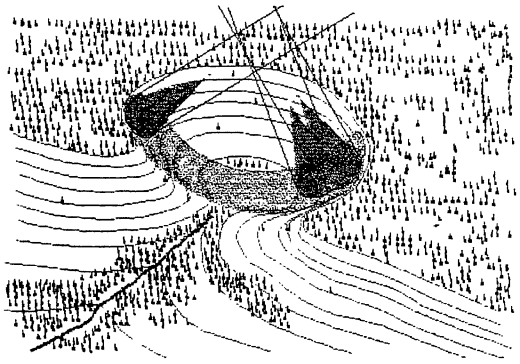

Figure 6. Carlina design using the curved shape of the ground.

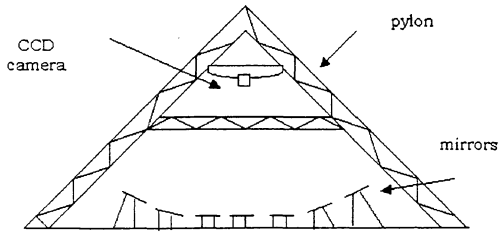

Figure 7. Carlina possible precursor. The primary diluted curved mirror is carried by fixed tripods. The aberration corrector and the pupil densifier are fixed on a 20 to 30 m high pylon structure. This pylon ensures the light recombination and allows the observation of stars up to 4 hours.

natural curved shape of the ground as a stable substrate carrying elements of a spherical mirror, in the form of an exploded or sparse mosaïc. Sperical mirror elements of 20 to 80 cm size, arrayed at 1 meter interval and carried by stable fixed tripods can be efficiently utilized according to the hypertelescope principle. This design requires an aberration corrector such as a Mertz corrector fixed on a 20 to 30 m high pylon. A 5-15 meters baseline is interesting for a first hypertelescope instrument. This Carlina-like design (Fig.7), beginning with 7 telescopes (the first ring and central obstruction), may be extended to 19 and 37 telescopes for a better (u,v) coverage. In a first step, the observations would be only available in a speckle mode if the sub-apertures diameters are smaller than 25 cm in visible or 60 cm in the K band. Addition of low order adaptive optics (only piston and tip-tilt corrections) would allow observation with a coronagraphic mode. The densification may be achieved with a pair of micro-lens arrays. This Carlina precursor is under study at the Haute Provence Observatory.

5. CONCLUSION

The pupil densifier is an optimization of (u,v) coverage for all interferometers. The laboratory and sky results confirmed the snapshot imaging possibilities with hypertelescopes. This densification method using two micro-lens arrays, increases noticeably the image quality and is easily controllable. The field of view is limited to the ZOF, the non-aliased field of view of the interferometer but may be adapted to the required observation with a modular densifier. Densified pupil imaging can be more efficient in terms of magnitude limitation than a classical interferometer. Coronagraphic and spectroscopic implementations are possible. Numerical simulations show that the resulting densified images may be used for spectroscopic and coronagraphic implementations with a focal mask such as the FQPM and such methods may be appropriate for the research and detection of exoplanets. This test is only a miniature version of hypertelescopes but announces interesting observation methods : various densified pupil implementations are possible such as a ground based Carlina design. Space version with less than forty small free-flyers may have powerful observing characteristics if coupled to a coronagraph. This last concept is being further explored in our group.

REFERENCES

Bensammar S., Gex, F., Horville, D., et al., 2000, Next Generation Space Telescope Science and Technology, ASP Conference Series, Vol. 207, 412

Gillet S. et al. 2001, CR. Acad. Sci. Paris, t. ,2, Serie IV, p. 27-33

Gilmozzi R. et al., 1998, SPIE, 3352,778

Heintz W.D., 1988, PASP, 100, 834

Labeyrie A., 1996, A&AS 118, 517

Pedretti E., Labeyrie A., Arnold L.,Thureau N., Lardière O., et al., 2000, A&AS 147, 285

Riaud P., Boccaletti A., Rouan D., Lemarquis F., & Labeyrie A., 2001, PASP 113, 1145

Riaud P., Gillet S., Labeyrie A., Boccaletti A., Schneider J., Rouan D., et al., 2001 Proc. "From Optical to Millimetric Interferometry", Liège Int. Astroph. Coll.

Riaud P., Boccaletti A., Gillet S., Arnold L., Lardière O. et al., 2002, A&A in preparation

Traub W.A, 1986, Applied optics, Vol. 25 No.4, 528